Original Article

Mediation of long-pulsed ultrasound enhanced microbubble recombinant tissue plasminogen activator thrombolysis in a rat model of platelet-rich thrombus

Shuxuan Zhou[1,2], Jinhua Li[3], Xianghui Chen[1], Bihan Huang[1], Dan Lu[4], Tao Zhang[1]

[1]Department of Cardiology, the First Affiliated Hospital of Jinan University, Guangzhou, China; [2]Cardiovascular Center, Hospital of Changan Dongguan, Dongguan, China; [3]Department of Ultrasound, the First Affiliated Hospital of Jinan University, Guangzhou, China; [4]Department of Neurology and Stroke Center, the First Affiliated Hospital of Jinan University, Guangzhou, China

Contributions: (I) Conception and design: X Chen, S Zhou; (II) Administrative support: T Zhang; (III) Provision of study materials or patients: X Chen; (IV) Collection and assembly of data: S Zhou, J Li, B Huang; (V) Data analysis and interpretation: S Zhou, X Chen, J Li, D Lu; (VI) Manuscript writing: All authors; (VII) Final approval of manuscript: All authors.

Correspondence to: Dr. Xianghui Chen, MD, PhD. Department of Cardiology, the First Affiliated Hospital of Jinan University, No. 613 Huangpu West Avenue, Guangzhou 510630, China. Email: armydoctorchen@163.com.

Background: Ultrasound (US)-enhanced microbubble (MB) therapy has been investigated as a therapeutic technique to facilitate the thrombolysis for the treatment of pericardial and microvascular obstruction. This study sought to assess the therapeutic effects of long-pulsed US-assisted MB-mediated recombinant tissue plasminogen activator (rt-PA) thrombolysis in a rat model of platelet-rich thrombus.

Methods: Ferric chloride (10%) was used to induce total arterial occlusion before formation of platelet-rich thrombi. Therapeutic long-tone-burst US (1 MHz, 0.6 MPa, 1,000-μs pulse length) was used, and 2.9×10^9/mL of lipid MBs and 1 mg/mL of rt-PA were infused. Subsequently, 42 Sprague-Dawley (SD) male rats were randomly divided into seven groups: (I) control; (II) rt-PA; (III) high duty cycle US + MB; (IV) low duty cycle US + rt-PA; (V) high duty cycle US + rt-PA; (VI) low duty cycle US + rt-PA + MB; and (VII) high duty cycle US + rt-PA + MB. The recanalization grades were evaluated after 20 minutes' treatment.

Results: Compared to the control, there was significant improvement in recanalization in the US + rt-PA groups (P=0.01 *vs.* control), US (low duty cycle) + rt-PA + MB (P=0.003 *vs.* control) and US (high duty cycle) + rt-PA + MB (P<0.001 *vs.* control) groups, in which recanalization was successfully achieved in all rats.

Conclusions: Long-pulsed US-enhanced MB-mediated rt-PA thrombolysis offered a powerful approach in the treatment of platelet-rich thrombus.

Keywords: Therapeutic thrombolysis; microbubble (MB); tissue plasminogen activator; ultrasonics; thrombosis

Submitted Aug 27, 2023. Accepted for publication Dec 29, 2023. Published online Feb 01, 2024.
doi: 10.21037/cdt-23-356
View this article at: https://dx.doi.org/10.21037/cdt-23-356

Introduction

In about 5–20% of patient who experience acute ST-segment elevation myocardial infarction (STEMI), successful revascularization of the epicardial coronary artery via percutaneous coronary intervention (PCI) cannot provide ideal microvascular reperfusion (1-3). Insufficient postprocedural reperfusion in myocardial capillaries is mainly caused by microvascular embolization and remains an important limitation that substantially reduces the beneficial effects of PCI. Microvascular embolization in patients is usually associated with a higher incidence of malignant arrhythmia, refractory heart failure, progressive left ventricular remodeling, and sudden death. Ultrasound (US)-enhanced microbubble (MB) therapy has been investigated as a useful technique for the lysis of occlusive thrombi in acute myocardial infarction (4,5)

and stroke (6). The therapeutic effects of US-assisted MB therapy have been found to facilitate thrombolysis under different experimental conditions: with recombinant tissue plasminogen activator (rt-PA) (7-9) and without rt-PA (10-12), with low frequency (40–500 kHz) (8,13) or high frequency (1–5 MHz) (14,15), and with targeted MB (5) or untargeted MB (16-18). Presently, the US used in clinic is usually short cycle (≤5 μs) (19). Long-pulsed duration (20 μs) US with MBs has become a valuable adjunct to reperfusion therapy for improving the effectiveness of sonothrombolysis therapy at a lower mechanical index (20). One clinical trial demonstrated that guided high mechanical index impulses with a 20-μs long-pulsed duration were able to prevent microvascular obstruction when coadministered with MB infusion (4). In other research, 30-μs pulse-length US was used to augment limb perfusion in patients with peripheral artery disease (21,22). Different from short-pulsed US, different long-pulse lengths (100–5,000 μs) of US were found to dissolve the microthrombi successfully *in vitro* (17). Further experiments showed long-tone-burst (5,000 μs)-assisted MB therapy to be an important strategy for the treatment of thrombotic microvascular obstruction *in vivo* (11). In a rodent model of microvascular obstruction, longer pulses (5,000 μs) caused greater MB cavitation followed by a more rapid microvascular flow restoration than did a 10-μs pulse US (23). Ultrahigh-speed imaging suggests that acoustic radiation forces (Bjerknes forces) can help mediate clot disruption under inertial cavitation conditions (24). The better treatment effects of a long-pulse duration of therapeutic impulses may be attributed to the sustained cavitation events that could restore both microvascular and epicardial flow, suggesting that long-pulse US is a promising direction for improving sonothrombolysis. rt-PA has been used for the treatment of STEMI as reperfusion therapy, but it does not provide an ideal therapeutic effect for arterial patency and is associated with disadvantages of cerebral or gastrointestinal bleeding (25). Transcatheter thrombolysis therapy decreases the risk of bleeding, but it's expensive and limited in large medical centers. Holland *et al.* demonstrated that both 120-kHz and 1-MHz pulsed or and continuous-wave US can enhance rt-PA thrombolysis (26) and that the initial lytic rate increases linearly with the duty cycle. US facilitates the transport of fibrinolytic enzymes into the clot by increasing the transport of reactants through a cavitation-related mechanism, and stable cavitation causing MB oscillation and microstreaming is critical to this process (8). This combined therapy has also been demonstrated to treat microvascular embolization and reperfuse the capillary network for infarction with no reflow (27).

US-assisted MB-mediated rt-PA thrombolysis therapy is still not widely used by the limitation of MB cavitation effect, because arterial total occlusion restricts blood flow and causes only a portion of the MBs arriving at the surface of the thrombi. In this study, a model of platelet-rich thrombus with total carotid arterial occlusion was established, and the synergistic effects of a novel 1,000 μs-pulse-length US, MB, and rt-PA were evaluated. We present this article in accordance with the ARRIVE reporting checklist (available at https://cdt.amegroups.com/article/view/10.21037/cdt-23-356/rc).

Highlight box

Key findings

- Long-pulsed ultrasound (US)-enhanced microbubble (MB)-mediated recombinant tissue plasminogen activator thrombolysis offered a powerful approach in the treatment of platelet-rich thrombus.

What is known and what is new?

- Long-tone-burst US enhanced MB thrombolysis has been investigated as a useful reperfusion therapy for thrombotic vascular obstruction.
- Our study shows the first time 1,000 μs long-pulsed US-mediated successful thrombolysis for platelet-rich thrombus in a totally occluded arterial model.

What is the implication, and what should change now?

- Long-pulsed US has great potentials for the treatment of microvascular obstruction and optimizing acoustic parameters should become the future direction of sonothrombolysis therapy.

Methods

Preparation of rt-PA and MB

rt-PA was stored at −80 ℃ in a freezer and was dilated with saline to a concentration of 1 mg/mL (28) before intravenous infusion. A dosage of 10 mg/kg was selected based on previous rat species studies (7,26). rt-PA was administered with a 10% bolus, which was followed by a 90% infusion with a syringe pump at a constant rate. Lipid MB (Sonovue, Bracco, Italy) was mixed with saline and then injected at a dose of 0.1 mL every 3 min. A Coulter counter showed the mean diameter of MB was 2.46±0.05 μm, with a concentration of $(2.99\pm0.19)\times10^9$/mL. To ensure the MBs arrived at the thrombi, visualization was performed

with a 18L7 imaging probe from an Aplio 500 US machine (Toshiba, Tokyo, Japan).

Animal model

Experiments were performed under a project license granted by ethics review board of Jinan University, Guangzhou, China (No. 44002100033991), in compliance with the institutional guidelines for the care and use of animals. To begin, 42 Sprague-Dawley (SD) male rats (n=6 for each group) weighing 290±30 g (age of 8–9 weeks) from the university animal center were anesthetized with pentobarbital sodium (40 mg/kg body weight, i.p). By using a computer based random order generator, all the rats were randomly numbered, and the groups were determined by a random draw. Rats were placed on a thermostat plate kept at a constant temperature of 37 ℃. The right external jugular vein was cannulated with a Polyethylene 50 tubing for infusion of rt-PA and MBs. The rat total carotid arterial occlusion model was established with 10% ferric chloride ($FeCl_3$) to induce platelet-rich thrombi (29). A segment of the left carotid artery was exposed using blunt dissection, and a plastic sheeting was placed beneath the carotid artery for protection of the surrounding tissues. A piece of paper (1 cm × 1 cm) saturated with 10% $FeCl_3$ solution was placed between the carotid artery and plastic sheeting to form thrombi (Figure S1). After 10 min of exposure, the filter paper and plastic sheeting were both removed.

The peak systolic velocity (PSV) was measured just proximal to the site of the injury in the left carotid artery with the Aplio 500 US machine. For reflection of the distal arterial resistance, the resistance index (RI) was derived with the following equation: RI = (PSV – diastolic flow velocity)/PSV. The two-dimensional (2D) and pulse-wave Doppler images of the left carotid artery at three different stages (baseline, thrombus, thrombolysis) were collected. No blood flow in Doppler US implied successful total occlusion of the carotid artery. Carotid arterial recanalization grade was assessed according to the following scheme: no flow across the lesion, grade 0; arterial stenosis >50%, grade I; residual arterial stenosis <50%; and complete recanalization, grade II. Individuals who died from anesthetic accident were excluded from our study.

Therapeutic US

A 1-MHz single-element transducer (A302S, Olympus, Tokyo, Japan) driven by a function generator (33250A, Agilent Technologies, Inc., Santa Clara, CA, USA) and a power amplifier (2200L, Electronics & Innovation, Rochester, NY, USA) was used to generate the therapeutic US (Figure S2). Because carotid arteries of the rats are superficial and because there is less attenuation for the application of US, 0.6 MPa (peak negative pressure) was used. Most of the recent related studies used 10- to 30-μs pulse lengths (4,20,21); however, the use of 5,000 μs has also drawn considerable attention (11,23), and therefore a 1,000-μs pulse length was selected for this investigation. Subsequently, 1-MHz US was delivered with two different duty cycles: 0.03% (pulse interval 3 s) and 10% (pulse interval 10 ms). When platelet-rich thrombus was successfully induced by $FeCl_3$, the transducer was gently placed vertically above the left carotid artery. We made sure that the thrombi were entirely covered by therapeutic US before we gently moved the probe up and down.

Treatment protocol

A protocol was prepared before the study without registration. SD rats were randomly divided into seven groups (n=6 for each group): (I) control; (II) rt-PA; (III) high duty cycle US + MB; (IV) low duty cycle US + rt-PA; (V) high duty cycle US + rt-PA; (VI) low duty cycle US + rt-PA + MB; and (VII) high duty cycle US + rt-PA + MB. n=6 for each group, and the estimation of sample size was based on a previous unpublished study. For all groups, the 2D and pulse-wave Doppler images of three different stages (baseline, thrombus, thrombolysis) were collected (Figure S3). The PSV, RI and arterial recanalization grade were calculated (Tables S1,S2). During the allocation, the conduct of the experiment, the outcome assessment, and the data analysis, were completed without the knowledge of each other.

Histology

Finally, rats were sacrificed via an overdose of potassium chloride, and hematoxylin and eosin (HE) staining was performed to analyze the effects of long-tone-burst US. The carotid arterial segment exposed to therapeutic US was selected, and the territory exposed to therapeutic US was sampled for histology. The magnification factor was 100×, and the representative pictures were selected.

Statistical analysis

SPSS 26.0 (IBM Corp., Armonk, NY, USA) was used

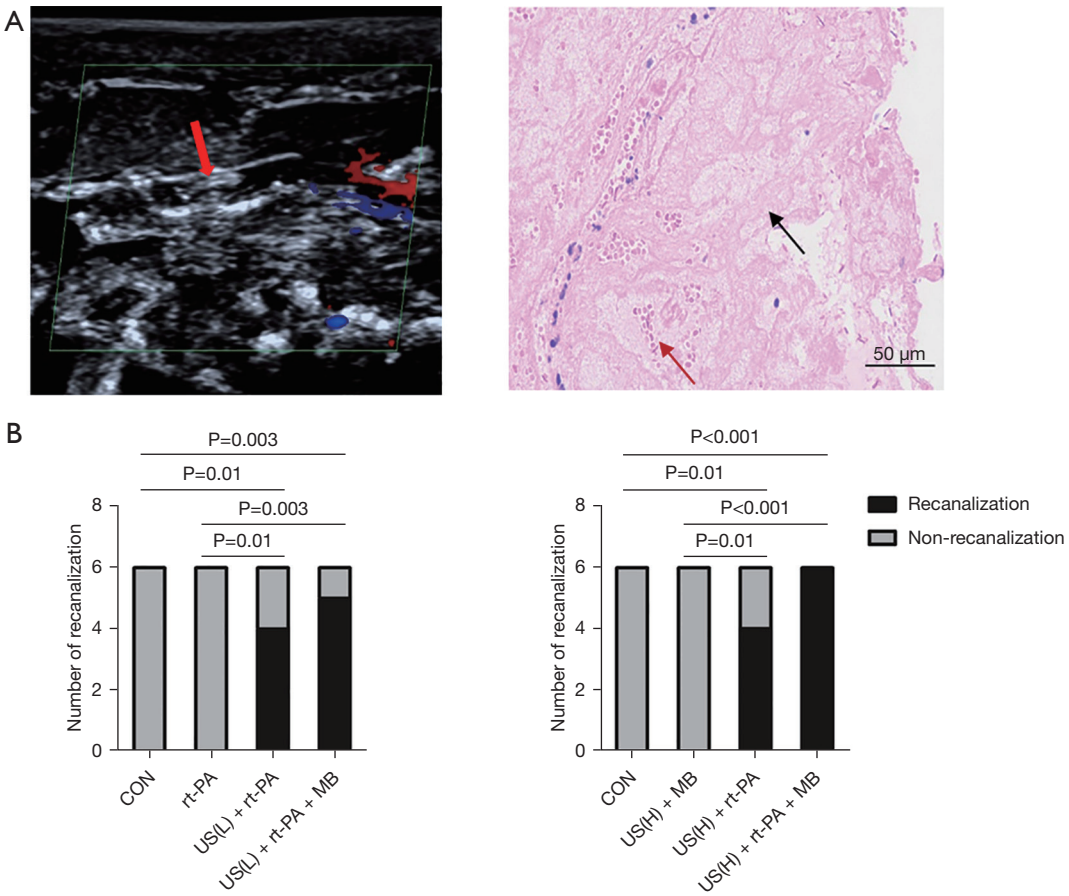

Figure 1 Platelet-rich thrombus and the thrombolytic effects. (A) Platelet-rich thrombi induced by 10% $FeCl_3$ solution in a rat model. (Left) the carotid artery was totally occluded by the fresh thrombi (red arrow). (Right) hematoxylin and eosin staining showed that the fresh platelet-rich thrombi were full of insoluble fibrous tissue, forming dense clots (black arrow) with only a small number of red blood cells (red arrow). (B) Recanalization after thrombolytic therapies. (Left) rt-PA showed no thrombolytic effects, but low duty cycle US + rt-PA showed good thrombolysis. (Right) high duty cycle US + rt-PA + MB showed the best thrombolytic effects. n=6 for each group. CON, control; rt-PA, recombinant tissue plasminogen activator; US(L), low duty cycle ultrasound; MB, microbubble; US(H), high duty cycle ultrasound; US, ultrasound.

for statistical analysis, and the PSV values are expressed as the mean ± standard deviation. One-way analysis of variance was used to compare differences within groups, the Bonferroni *post hoc* test was used for the comparison of the differences between groups, and the Fisher exact test was used to analyze the recanalization rate. A two-sided P value <0.05 was considered significant.

Results

A successful rat model of total carotid arterial occlusion was induced with a 10% $FeCl_3$ solution. As shown in *Figure 1A*, color Doppler confirmed the carotid artery was totally occluded by the fresh thrombus. Pathology showed the thrombi were full of insoluble fibrous tissue, forming dense clots, with only a small number of red blood cells. *Figure 1B* shows how the pure administration of rt-PA did not have thrombolytic effect for the fresh platelet-rich thrombi. However, when assisted with low duty cycle US, rt-PA showed good thrombolysis (P=0.01 *vs.* control). Moreover, there was a tendency toward an increase in thrombolytic rate when MBs were further added. Under the high duty cycle US condition, pure MBs did not show enough capacity to dissolving platelet-rich thrombi. However, US combined with rt-PA showed apparent thrombolysis (P=0.01 *vs.* control). Furthermore, there was an increase in the thrombolytic rate

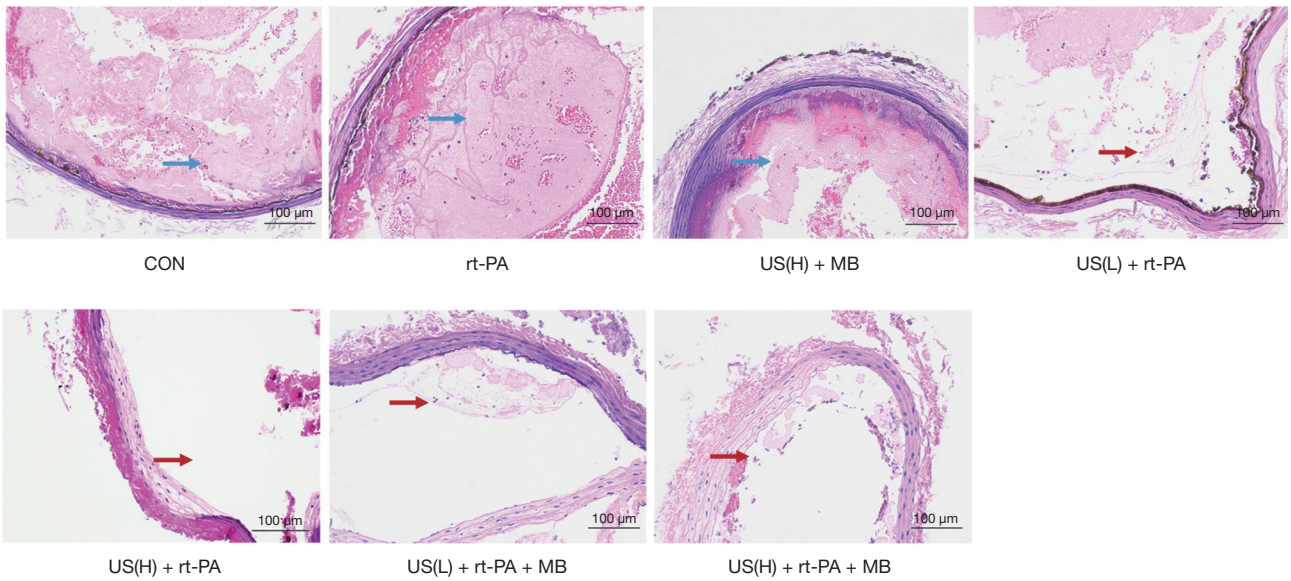

Figure 2 Hematoxylin and eosin staining of the platelet-rich thrombi in rats post thrombolytic therapy (magnification factor 100×). There was abundant insoluble fibrous tissue in the vessels, forming dense clots in control, rt-PA, and high duty-cycle ultrasound + microbubble groups. Only a small amount of insoluble latticed fibrous tissues was found in the ultrasound + rt-PA + microbubble groups. The US(L) + rt-PA group was in the intermediate stage. The blue arrow indicates unsuccessful thrombolysis, and the red arrow indicates successful thrombolysis. CON, control; rt-PA, recombinant tissue plasminogen activator; US(H), high duty cycle ultrasound; MB, microbubble; US(L), low duty cycle ultrasound.

in the US + rt-PA + MB group (P<0.001 *vs.* control).

HE staining of formalin-preserved arterial slices confirmed the successful establishment of the platelet- rich thrombi. Most of the thrombi remained intact in the control, rt-PA, and US + MB groups, as illustrated in *Figure 2*. A fairly large percent of thrombi was dissolved in the low duty cycle US + rt-PA and high duty cycle US + rt-PA groups. The thrombolytic effects were further intensified in the low duty cycle US + rt-PA + MB and high duty cycle US + rt-PA + MB groups.

Discussion

In this study, platelet-rich thrombi in a rat model of total carotid arterial occlusion was made, and the synergistic effects of long-pulsed US, rt-PA, and MB were evaluated. $FeCl_3$ with different concentrations (2–60%) has been widely used to induce arterial thrombosis in a variety of species (30). $FeCl_3$ causes endothelial injury, platelet aggregation, thrombin release, and fibrin deposition, along with dense-structure thrombus. The intrinsic components of $FeCl_3$-induced thrombus consist of activated platelets, fibrin, and red blood cells, which is a similar composition to that of human coronary arteries after acute myocardial infarction. In our experiment, 10% $FeCl_3$ was used with an exposure time of 10 min. Color Doppler confirmed total occlusion in left carotid arteries in all the rats, and the success rate of the arterial thrombosis model was 100%. Therefore, our procedure is a simple, sensitive, and reproducible method of establishing platelet-rich thrombi in a rat model.

To our knowledge, this is the first study to show long-pulsed US-mediated successful thrombolysis for platelet-rich thrombus in a totally occluded arterial model. Most of the preliminary studies *in vitro* involve red blood cell-rich thrombi, with MBs being continuously infused and arriving at the location of the thrombus formation (8,9). Therefore, a persistent MB cavitation effect can lead to thrombolysis while therapeutic US is delivered without attenuation. However, new-formed thrombi usually cause arterial total occlusion and restrict blood flow in patients with STEMI, lead to only a portion of the MBs arriving at the surface of the thrombi. A decreased MB cavitation effect often result in the failures of sonothrombolysis, especially for the platelet-rich thrombi with a dense structure. In our study, ~0.5 mL of MBs were used, and the synergistic effects of MBs and rt-PA showed excellent thrombolytic capacity

under long-pulsed acoustic conditions.

rt-PA is an important treatment drug and has been approved by the US Food and Drug Administration (FDA) for ischemic stroke (31). The stirring effect caused by acoustic microstreaming is of the main mechanisms underlying the action of US-enhanced MB-mediated rt-PA thrombolysis since it facilitates the exposure of new binding sites for plasmin near the fibrin mesh, accelerates oscillating MBs, and promotes removal of fibrin degradation products away from the clot (8). Stable cavitation has been demonstrated to accelerate thrombolysis when US, rt-PA, and MB act synergistically (8) (Figure S4). In our study, pure administration of rt-PA did not cause patency of the occluded artery likely because the platelet-rich thrombi were quite solid. High duty cycle US (0.6 MPa) with MBs typically generates stable cavitation events; (17) therefore, the radiation forces from microstreaming are unable to completely dissolve the rigid thrombi. Additionally, MBs, acting synergistically with rt-PA, can improve the recanalization rate. In our study, the recanalization grade in the US + rt-PA + MB group was higher than that in the US + rt-PA group regardless of which duty cycle was used. The duty cycle dependence of 120-kHz US-enhanced thrombolysis was demonstrated in a human clot model (13). With this model, the lytic rate increased linearly with the increase of the duty cycle since the increase of duty cycle provides more sustained MB cavitation events that can accelerate thrombolysis. Our study found that in rats treated with a treatment of US + rt-PA + MB, the high duty cycle achieved a 100% recanalization rate after thrombolytic therapy. A recent study examined MBs undergoing inertial cavitation under 5,000-μs pulse-length US with high acoustic pressure (32). Under the long-tone-burst US excitation, MB oscillations activated the endothelial nitric oxide synthase (eNOS) pathway with nitro oxide playing a significant role, and blood reperfusion was improved (33). In a different study, the MB acoustic behaviors caused sustained enhancement of cellular and vascular permeability through a physical, cavitation-based mechanism of sonoporation (34). In our study, long-pulse-length US of 1,000 μs was used with MB-assisted rt-PA therapy and showed highly promising effects in dissolving clots. The passive detection of MB cavitation should be monitored for further clarification of the thrombolytic mechanisms with long-tone-burst US.

Strengths and limitations

First of all, the thrombus in our model was full of fresh platelets with dense structure, resistant to pure intravenous administration of rt-PA. Moreover, a novel 1,000 μs-pulse-length was used, and this long-pulsed US showed powerful thrombolytic effects in a rat model of platelet-rich thrombus. Third, the successful thrombolysis in the total carotid arterial occlusion model showed this combined therapy has great potentials to overcome the shortcoming of traditional US-assisted MB-mediated rt-PA therapy—limitation of cavitation effect. The main limitation of our study is the detection of cavitation activities (Figure S5) was not recorded. Further studies are needed to clarify of the intrinsic mechanisms of this promising combined therapy.

Conclusions

Long-tone-burst US-assisted MB-enhanced rt-PA therapy showed successful thrombolytic effects for platelet-rich thrombus in rats with total arterial occlusion and may offer a powerful approach for the treatment for arterial thrombosis.

Acknowledgments

Funding: This study was funded by the National Natural Science Foundation of China (grant No. 81400266 to X. Chen) and the counterpart fund from the First Affiliated Hospital of Jinan University, Guangzhou, China (grant No. 501134 to X. Chen). The funders have no role in the design and conduct of the study; collection, analysis, and interpretation of the data; preparation, or approval of the manuscript.

Footnote

Reporting Checklist: The authors have completed the ARRIVE reporting checklist. Available at https://cdt.amegroups.com/article/view/10.21037/cdt-23-356/rc

Data Sharing Statement: Available at https://cdt.amegroups.com/article/view/10.21037/cdt-23-356/dss

Peer Review File: Available at https://cdt.amegroups.com/article/view/10.21037/cdt-23-356/prf

Conflicts of Interest: All authors have completed the ICMJE uniform disclosure form (Available at https://cdt.amegroups.com/article/view/10.21037/cdt-23-356/coif). The authors have no conflicts of interest to declare.

Ethical Statement: The authors are accountable for all aspects of the work in ensuring that questions related to the accuracy or integrity of any part of the work are appropriately investigated and resolved. Experiments were performed under a project license granted by ethics review board of Jinan University, Guangzhou, China (No. 44002100033991), in compliance with the institutional guidelines for the care and use of animals.

References

1. Ndrepepa G. Angiographic coronary no-reflow after primary percutaneous coronary intervention - a combination of an insensitive diagnostic method, inappropriate timing and rushed judgement. EuroIntervention 2023;19:e368-70.
2. Niccoli G, Burzotta F, Galiuto L, et al. Myocardial no-reflow in humans. J Am Coll Cardiol 2009;54:281-92.
3. Konijnenberg LSF, van Royen N. Perilipin 2 - another piece in the big jigsaw puzzle of coronary no reflow. Eur Heart J Acute Cardiovasc Care 2021;10:643-4.
4. Mathias W Jr, Tsutsui JM, Tavares BG, et al. Diagnostic Ultrasound Impulses Improve Microvascular Flow in Patients With STEMI Receiving Intravenous Microbubbles. J Am Coll Cardiol 2016;67:2506-15.
5. Xie F, Lof J, Matsunaga T, et al. Diagnostic ultrasound combined with glycoprotein IIb/IIIa-targeted microbubbles improves microvascular recovery after acute coronary thrombotic occlusions. Circulation 2009;119:1378-85.
6. Alexandrov AV, Demchuk AM, Burgin WS, et al. Ultrasound-enhanced thrombolysis for acute ischemic stroke: phase I. Findings of the CLOTBUST trial. J Neuroimaging 2004;14:113-7.
7. Hitchcock KE, Ivancevich NM, Haworth KJ, et al. Ultrasound-enhanced rt-PA thrombolysis in an ex vivo porcine carotid artery model. Ultrasound Med Biol 2011;37:1240-51.
8. Datta S, Coussios CC, Ammi AY, et al. Ultrasound-enhanced thrombolysis using Definity as a cavitation nucleation agent. Ultrasound Med Biol 2008;34:1421-33.
9. Goyal A, Yu FTH, Tenwalde MG, et al. Inertial Cavitation Ultrasound with Microbubbles Improves Reperfusion Efficacy When Combined with Tissue Plasminogen Activator in an In Vitro Model of Microvascular Obstruction. Ultrasound Med Biol 2017;43:1391-400.
10. Black JJ, Yu FT, Schnatz RG, et al. Effect of Thrombus Composition and Viscosity on Sonoreperfusion Efficacy in a Model of Micro-Vascular Obstruction. Ultrasound Med Biol 2016;42:2220-31.
11. Pacella JJ, Brands J, Schnatz FG, et al. Treatment of microvascular micro-embolization using microbubbles and long-tone-burst ultrasound: an in vivo study. Ultrasound Med Biol 2015;41:456-64.
12. Belcik JT, Mott BH, Xie A, et al. Augmentation of limb perfusion and reversal of tissue ischemia produced by ultrasound-mediated microbubble cavitation. Circ Cardiovasc Imaging 2015;8:e002979.
13. Meunier JM, Holland CK, Lindsell CJ, et al. Duty cycle dependence of ultrasound enhanced thrombolysis in a human clot model. Ultrasound Med Biol 2007;33:576-83.
14. Cintas P, Nguyen F, Boneu B, et al. Enhancement of enzymatic fibrinolysis with 2-MHz ultrasound and microbubbles. J Thromb Haemost 2004;2:1163-6.
15. Belcik JT, Davidson BP, Xie A, et al. Augmentation of Muscle Blood Flow by Ultrasound Cavitation Is Mediated by ATP and Purinergic Signaling. Circulation 2017;135:1240-52.
16. Prokop AF, Soltani A, Roy RA. Cavitational mechanisms in ultrasound-accelerated fibrinolysis. Ultrasound Med Biol 2007;33:924-33.
17. Leeman JE, Kim JS, Yu FT, et al. Effect of acoustic conditions on microbubble-mediated microvascular sonothrombolysis. Ultrasound Med Biol 2012;38:1589-98.
18. Tu J, Hwang JH, Matula TJ, et al. Intravascular inertial cavitation activity detection and quantification in vivo with Optison. Ultrasound Med Biol 2006;32:1601-9.
19. Porter TR. The utilization of ultrasound and microbubbles for therapy in acute coronary syndromes. Cardiovasc Res 2009;83:636-42.
20. Wu J, Xie F, Kumar T, et al. Improved sonothrombolysis from a modified diagnostic transducer delivering impulses containing a longer pulse duration. Ultrasound Med Biol 2014;40:1545-53.
21. Mason OR, Davidson BP, Sheeran P, et al. Augmentation of Tissue Perfusion in Patients With Peripheral Artery

Disease Using Microbubble Cavitation. JACC Cardiovasc Imaging 2020;13:641-51.
22. Villanueva FS, Chen X. Complex Highways on the Translational Roadmap for Therapeutic Ultrasound-Targeted Microbubble Cavitation: Where Are We Now? JACC Cardiovasc Imaging 2020;13:652-4.
23. Yu FTH, Amjad MW, Mohammed SA, et al. Effect of Ultrasound Pulse Length on Sonoreperfusion Therapy. Ultrasound Med Biol 2023;49:152-64.
24. Chen X, Leeman JE, Wang J, et al. New insights into mechanisms of sonothrombolysis using ultra-high-speed imaging. Ultrasound Med Biol 2014;40:258-62.
25. Ma H, Campbell BCV, Parsons MW, et al. Thrombolysis Guided by Perfusion Imaging up to 9 Hours after Onset of Stroke. N Engl J Med 2019;380:1795-803.
26. Holland CK, Vaidya SS, Datta S, et al. Ultrasound-enhanced tissue plasminogen activator thrombolysis in an in vitro porcine clot model. Thromb Res 2008;121:663-73.
27. Xie F, Slikkerveer J, Gao S, et al. Coronary and microvascular thrombolysis with guided diagnostic ultrasound and microbubbles in acute ST segment elevation myocardial infarction. J Am Soc Echocardiogr 2011;24:1400-8.
28. Shaw GJ, Sperling M, Meunier JM. Long-term stability of recombinant tissue plasminogen activator at -80 C. BMC Res Notes 2009;2:117.
29. Wang X, Xu L. An optimized murine model of ferric chloride-induced arterial thrombosis for thrombosis research. Thromb Res 2005;115:95-100.
30. Wang X, Smith PL, Hsu MY, et al. Murine model of ferric chloride-induced vena cava thrombosis: evidence for effect of potato carboxypeptidase inhibitor. J Thromb Haemost 2006;4:403-10.
31. Broderick JP, Palesch YY, Demchuk AM, et al. Endovascular therapy after intravenous t-PA versus t-PA alone for stroke. N Engl J Med 2013;368:893-903.
32. Chen X, Chen X, Wang J, et al. Dynamic Behavior of Polymer Microbubbles During Long Ultrasound Tone-Burst Excitation and Its Application for Sonoreperfusion Therapy. Ultrasound Med Biol 2023;49:996-1006.
33. Yu FTH, Chen X, Straub AC, et al. The Role of Nitric Oxide during Sonoreperfusion of Microvascular Obstruction. Theranostics 2017;7:3527-38.
34. Helfield B, Chen X, Watkins SC, et al. Biophysical insight into mechanisms of sonoporation. Proc Natl Acad Sci U S A 2016;113:9983-8.

Cite this article as: Zhou S, Li J, Chen X, Huang B, Lu D, Zhang T. Mediation of long-pulsed ultrasound enhanced microbubble recombinant tissue plasminogen activator thrombolysis in a rat model of platelet-rich thrombus. Cardiovasc Diagn Ther 2024;14(1):51-58. doi: 10.21037/cdt-23-356

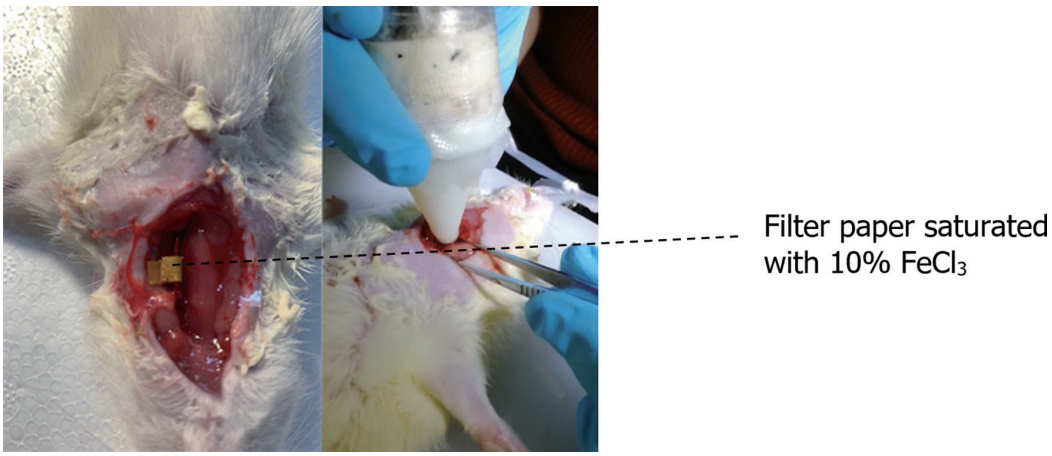

Figure S1 The establishment of a rat model of platelet-rich thrombi. The rat carotid artery was exposed to 10% ferric chloride ($FeCl_3$) for 10 minutes. A piece of filter paper (1 cm × 1 cm) saturated with 10% $FeCl_3$ solution was placed between the carotid artery and a plastic sheeting to form thrombus. 1 MHz therapeutic ultrasound was delivered from a single-element transducer (A302S) for 20 minutes.

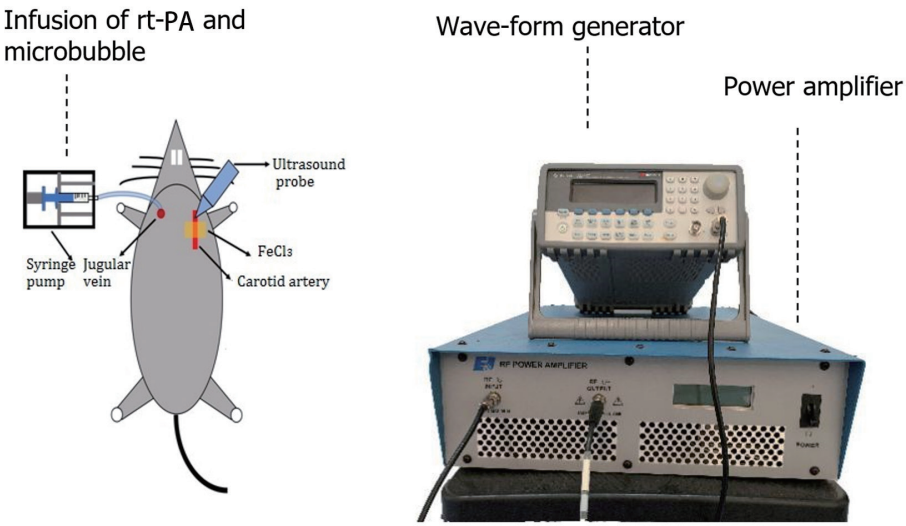

Figure S2 Long-pulsed ultrasound enhanced microbubble mediated recombinant tissue plasminogen activator (rt-PA) thrombolysis. Recombinant tissue plasminogen activator and microbubble were infused through the right external jugular vein of the rats. Therapeutic ultrasound (1 MHz, 0.6 MPa) with 1,000 μs pulse-length was delivered from an arbitrary function generator (33250A) and intensified by a power amplifier (EI 2200L). $FeCl_3$, ferric chloride.

https://dx.doi.org/10.21037/cdt-23-356

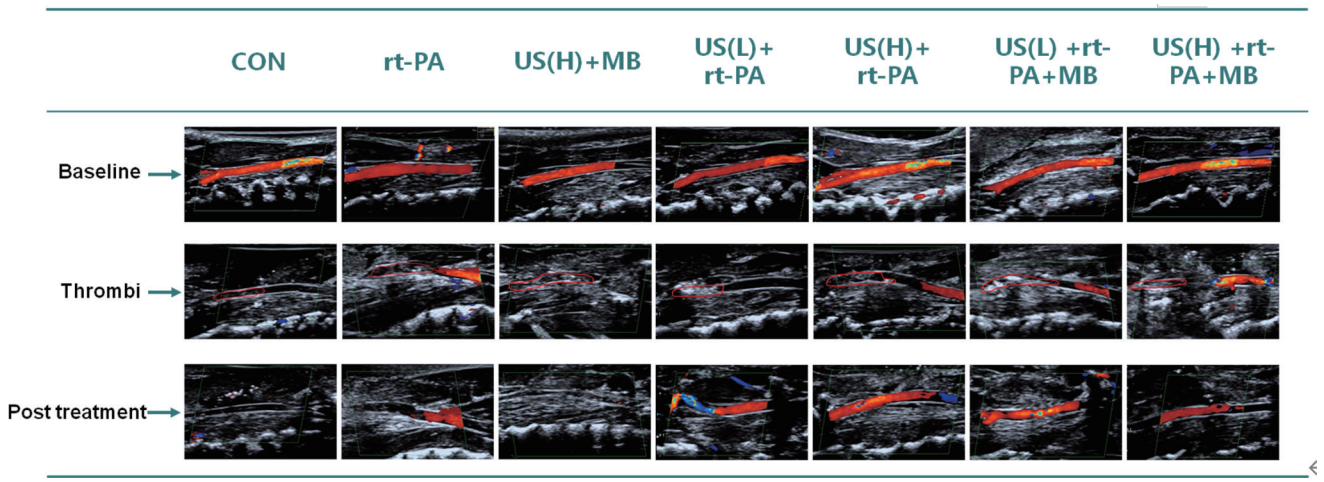

Figure S3 Pulse-wave Doppler images of rats' carotid artery at three different stages (baseline, thrombi, thrombolysis). n=6 for each group. CON, control; rt-PA, recombinant tissue plasminogen activator; US, ultrasound; US(H), high duty-cycle (10%) ultrasound; US(L), low duty-cycle (0.03%) ultrasound; MB, microbubble.

Table S1 The peak systolic velocity (PSV) and resistance index (RI) at baseline stage in different groups before thrombi formation. Data are expressed as the mean ± standard deviation (n=6 for each group)

Index/Group	CON	rt-PA	US(H) + MB	US(L) + rt-PA	US(H) + rt-PA	US(L) + rt-PA + MB	US(H) + rt-PA + MB	P value
Peak systolic velocity (cm/s)	59.08±13.70	56.77±2.90	47.38±6.57	57.88±17.32	57.08±12.15	41.73±9.23	48.06±15.77	0.171
Resistance index	0.80±0.04	0.80±0.04	0.89±0.09	0.83±0.04	0.86±0.04	0.81±0.06	0.83± 0.06	0.053

CON, control; rt-PA, recombinant tissue plasminogen activator; US, ultrasound; US(H), high duty-cycle (10%) ultrasound; US(L), low duty-cycle (0.03%) ultrasound; MB, microbubble.

Table S2 Recanalization grading after thrombolytic therapies

Recanalization grading	CON	rt-PA	US(H) + MB	US(L) + rt-PA	US(H) + rt-PA	US(L) + rt-PA + MB	US(H) + rt-PA + MB
0	6	6	6	2	2	1	–
I	–	–	–	2	–	1	–
II	–	–	–	2	4	4	6

No recanalization was observed in control, recombinant tissue plasminogen activator and ultrasound+ microbubble groups. Using long pulsed ultrasound (1,000 μs) and recombinant tissue plasminogen activator (1 mg/mL), high duty-cycle ultrasound caused 4/6 grade II for recanalization. When microbubble was added, high duty-cycle ultrasound with recombinant tissue plasminogen activator successfully achieved all grade II of recanalization. CON, control; rt-PA, recombinant tissue plasminogen activator; US, ultrasound; US(H), high duty-cycle (10%) ultrasound; US(L), low duty-cycle (0.03%) ultrasound; MB, microbubble.

https://dx.doi.org/10.21037/cdt-23-356

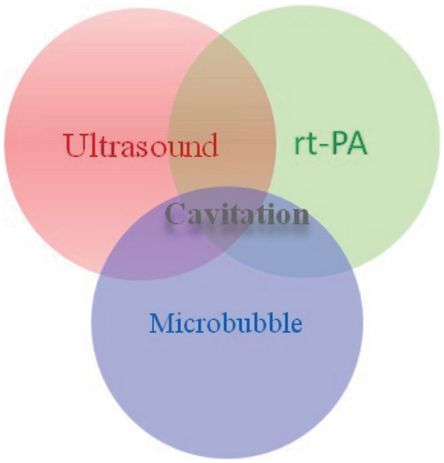

Figure S4 Synergistic effects of ultrasound, recombinant tissue plasminogen activator (rt-PA) and microbubbles through the cavitation mechanism.

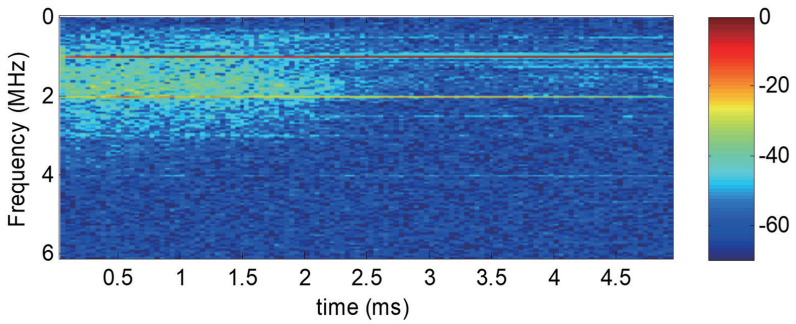

Figure S5 The passive detection of microbubble cavitation during the sonothrombolysis. A 2.25 MHz transducer, confocally aligned with the treatment transducer focal territory, was used to passively detect scattered energy. The signal was amplified by 10 dB and digitized by an oscilloscope at 50 MHz sampling frequency. A time frequency analysis was performed over the pulse duration, using a 100 μs sliding window with 60% overlapping. And the frequency content of the received signal at each time point is displayed as a function of time.

https://dx.doi.org/10.21037/cdt-23-356